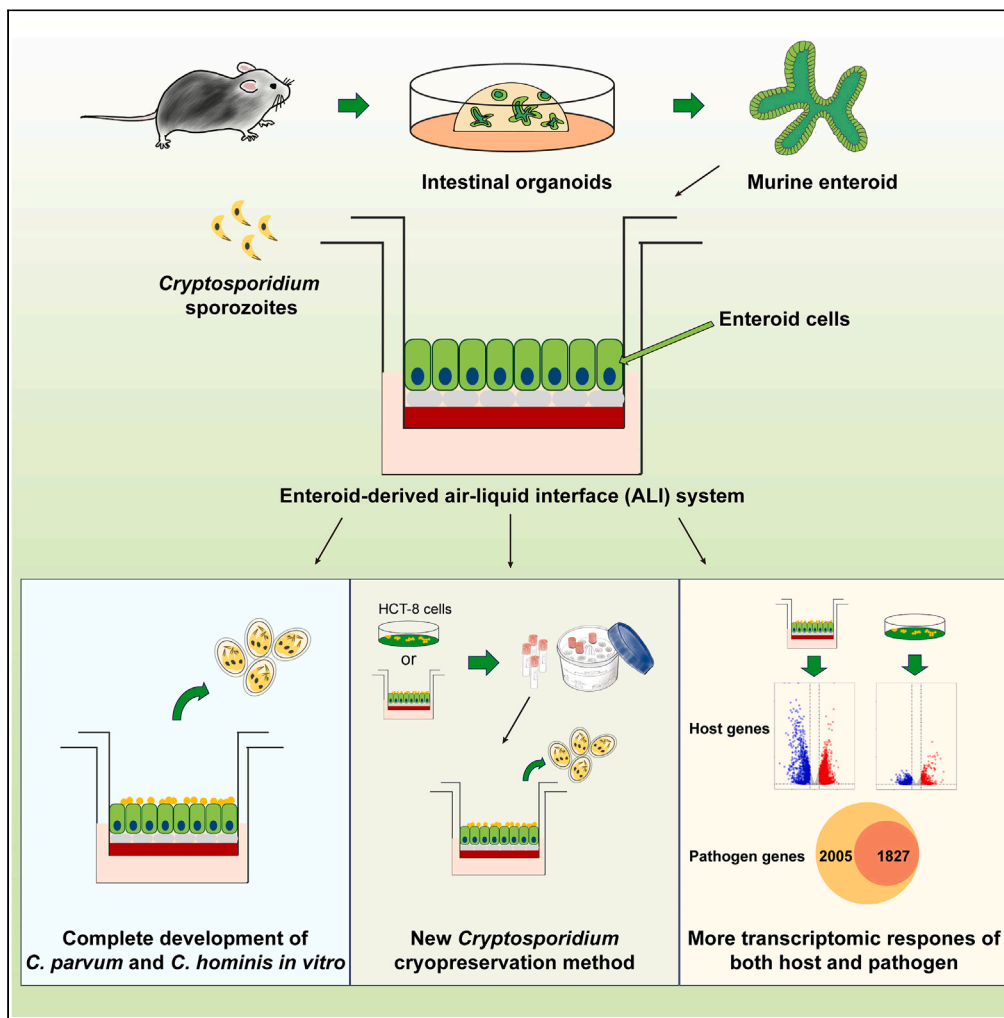


Article

Cultivation, cryopreservation, and transcriptomic studies of host-adapted *Cryptosporidium parvum* and *Cryptosporidium hominis* using enteroids



Miner Deng, Tianyi Hou, Jie Zhang, ..., Lihua Xiao, Yaoyu Feng, Yaqiong Guo

lxiao1961@gmail.com (L.X.)  
yyfeng@scau.edu.cn (Y.F.)  
guoyq@scau.edu.cn (Y.G.)

Highlights

Procedures for culturing *Cryptosporidium* using murine enteroids are simplified

The system allows complete development of both *C. parvum* and divergent *C. hominis*

Enteroids infected with *C. hominis* induce strong transcriptomic responses

A new *Cryptosporidium* cryopreservation method is developed using enteroid cultures



## Article

Cultivation, cryopreservation, and transcriptomic studies of host-adapted *Cryptosporidium parvum* and *Cryptosporidium hominis* using enteroids

Miner Deng,<sup>1,2</sup> Tianyi Hou,<sup>1,2</sup> Jie Zhang,<sup>1</sup> Xinjie Mao,<sup>1</sup> Fuxian Yang,<sup>1</sup> Yanting Wei,<sup>1</sup> Yongping Tang,<sup>1</sup> Wanting Zeng,<sup>1</sup> Wanyi Huang,<sup>1</sup> Na Li,<sup>1</sup> Lihua Xiao,<sup>1,3,\*</sup> Yaoyu Feng,<sup>1,\*</sup> and Yaqiong Guo<sup>1,\*</sup>

## SUMMARY

***Cryptosporidium hominis* and *Cryptosporidium parvum* are major causes of severe diarrhea. Comparative studies of them are hampered by the lack of effective cultivation and cryopreservation methods, especially for *C. hominis*. Here, we describe adapted murine enteroids for the cultivation and complete development of host-adapted *C. parvum* and *C. hominis* subtypes, producing oocysts infectious to mice. Using the system, we developed a cryopreservation method for *Cryptosporidium* isolates. In comparative RNA-seq analyses of *C. hominis* cultures, the enteroid system generated significantly more host and pathogen responses than the conventional HCT-8 cell system. In particular, the infection was shown to upregulate PI3K-Akt, Ras, TNF, NF- $\kappa$ B, IL-17, MAPK, and innate immunity signaling pathways and downregulate host cell metabolism, and had significantly higher expression of parasite genes involved in oocyst formation. Therefore, the enteroid system provides a valuable tool for comparative studies of the biology of divergent *Cryptosporidium* species and isolates.**

## INTRODUCTION

Cryptosporidiosis is an important cause of severe diarrhea in humans, responsible for major waterborne epidemics in high-income countries and childhood malnutrition and death in low- and middle-income countries.<sup>1,2</sup> *Cryptosporidium hominis* and *Cryptosporidium parvum* are two main species responsible for human cryptosporidiosis.<sup>3</sup> Between them, *C. hominis* has a narrow host range, being found in mainly equine animals in addition to humans and other primates, while *C. parvum* infects a broad range of animals including primates, ruminants, equine animals, and rodents.<sup>4</sup> The two also differ significantly in genomics and virulence.<sup>5,6</sup> In humans, *C. hominis* infection is associated with diarrhea, nausea, vomiting, general malaise, and increased intensity and duration of oocyst shedding, while *C. parvum* is associated with diarrhea only. The genomes of these two species are nearly 96% identical in nucleotide sequence, with several small deletions and one insertion in *C. hominis*.<sup>7</sup>

Within the two major human-pathogenic species, there are significant variations in phenotypic traits at the subtype family level.<sup>4</sup> Among the different subtype families of *C. parvum*, Ila and IId are the two major zoonotic ones commonly found in humans and farm animals. Between them, Ila subtypes are common in intensively farmed dairy calves, causing outbreaks of zoonotic cryptosporidiosis in most high-income countries.<sup>4</sup> In contrast, IId subtypes are more common in lambs and goat kids in Europe, Mideast countries and Oceania and in dairy calves in China and Sweden, causing mostly sporadic zoonotic infections in humans.<sup>8</sup> Similarly, *C. hominis* subtype families differ in host preference and virulence. In addition to the common Ia, Ib, Id, Ie, and If subtype families in humans, several new subtype families have been identified in equine animals (Ik) and nonhuman primates (Ii, Im, and In).<sup>4</sup> Currently, biological studies on *Cryptosporidium* spp. have mostly concentrated on *C. parvum* Ila subtypes, while the IId subtypes prevalent in some countries are rarely used.<sup>9</sup> In addition, studies of the biological characteristics of *C. hominis* are very limited because of the lack of easily accessible cultivation and animal models.<sup>9</sup>

Although several significant progresses, such as the development of potential treatments<sup>10</sup> and genetic modification tools,<sup>11</sup> have been made in recent years, we still have a rudimentary understanding of *Cryptosporidium* spp.<sup>12</sup> One of the most important reasons is the lack of effective and economic culture platform to support the complete life cycle of *Cryptosporidium* spp. and propagation of oocysts *in vitro*. Human adenocarcinoma cell lines (such as HCT-8 cells) are widely used in *in vitro* studies of *C. parvum*, but they support only partial development of the pathogen without the production of oocysts, the infective stage.<sup>13</sup> To support complete the development of *C. parvum* and maintain long-term cultures, several studies have reported the establishment of various 3D culture systems. However, these novel culture systems are

<sup>1</sup>State Key Laboratory for Animal Disease Control and Prevention, South China Agricultural University, Guangzhou, Guangdong, China

<sup>2</sup>These authors contributed equally

<sup>3</sup>Lead contact

\*Correspondence: lxiao1961@gmail.com (LX.), yfeng@scau.edu.cn (Y.F.), guoyq@scau.edu.cn (Y.G.)

<https://doi.org/10.1016/j.isci.2024.109563>



difficult to manipulate and require expensive and specialized equipment.<sup>13,14</sup> In addition, the HCT-8 cells used differ biologically from native epithelial cells in the intestine.

Organoids, products of the 3D culture of stem cells, retain the biological characteristics, unique markers and other functional properties of the native tissues.<sup>15</sup> Recent studies indicate that organoids derived from intestinal crypts can be used in drug screening, organ transplant, modeling of genetic diseases, and studies of host-pathogen interactions.<sup>16</sup> Heo et al. demonstrated that *C. parvum* could be cultured in human intestinal and lung organoids.<sup>17</sup> However, the culture system developed requires the microinjection of individual organoids, hampering its routine applications. More recently, Wilke et al. developed a new enteroid system for the complete development of *C. parvum*.<sup>18</sup> It grows stem cells digested from the ileum in Transwells and uses an air liquid interface (ALI) to induce cell differentiation. The new enteroid system sustains the growth of Ila subtypes of *C. parvum*, leading to the generation of infective oocysts. Using human tissues, a similar ALI system has been established for the cultivation of one human *C. hominis* isolate.<sup>19</sup> However, none of the new and conventional systems have been used effectively in the cultivation of the *C. parvum* IId subtype family and nonhuman primate-adapted *C. hominis* subtypes.

Another major bottleneck of research progress is the lack of accessible cryopreservation of *Cryptosporidium* oocysts. Currently, researchers propagate *Cryptosporidium* spp. in laboratory animals every 2–6 months, which is labor-intensive and expensive. Recently, a cryopreservation method of *C. parvum* by freezing permeabilized oocysts in silica microcapillaries was reported.<sup>20</sup> To overcome the limited volume (~2  $\mu$ L oocyst suspension) of microcapillaries, the research group developed a modified cryopreservation protocol by using 'vitrification cassettes', and adapted it for the cryopreservation of *C. hominis* oocysts.<sup>21,22</sup> However, these methods require specialized equipment that is not available in most laboratories.

Here, we refined the procedures for the generation of murine enteroids and ALI cultures, including modifications of feeder cell induction, digestion of enteroids, and the medium used in the ALI culture. We have used the new ALI system in the cultivation of one *C. parvum* IId subtype and three nonhuman primate-adapted *C. hominis* subtypes. Based on the ALI culture system, we established a novel cryopreservation method of *C. parvum* for long-term maintenance of isolates. In addition, we compared transcriptomic responses in HCT-8 and ALI cultures infected with *C. hominis* through RNA-seq analysis. The new system supports the complete development of both *C. parvum* and nonhuman primate-adapted *C. hominis*, permits the cryopreservation of *Cryptosporidium* isolates, and allows comparative studies of the biology and host-pathogen interactions of multiple *Cryptosporidium* species and isolates in a controlled environment.

## RESULTS

### Development of an enteroid-derived ALI system for *C. parvum* cultivation

We generated enteroid stocks from intestinal crypts for establishing the ALI system (Figure 1A). The intestinal crypts isolated from the intestines of C57BL/6 mice looked initially like pellets (Figure 1B). After three days of culture, enteroids started to form, with budded crypt-like and villus-like domains (Figure 1B). The enteroids generated could be maintained in culture for over 6 months, and cryopreserved for future usage. Through one or more rounds of passages, numerous enteroids with few single cells or mesenchymal cells could be produced for establishing the ALI culture system.

Using the enteroids grown in Transwells, we adapted the ALI culture system following procedures described previously<sup>18</sup> with modifications of the medium used, the induction of feeding cells and the digestion of enteroids. The ALI cultures were infected with  $1 \times 10^5$  oocysts of the Ila-Waterborne isolate of *C. parvum* three days after the top medium was removed. Results of qPCR analysis showed that parasite growth was amplified by ~70-fold from the initial infection dose. The parasite load peaked at DPI 3 (Figure 1C). The amplification of ALI cultures infected with  $2 \times 10^5$  oocysts showed a similar trend. Histological examination of the ALI cultures revealed the presence of parasites on the surface of ALI monolayers (Figure 1D). Immunofluorescent staining of the ALI monolayers infected with purified sporozoites using antibodies against developing stages (Sporo-Glo) and oocysts (Crypt-a-Glo) confirmed the production of oocysts in the ALI cultures (Figure 1E).

### The ALI system allowed the full development of the IId subtype of *C. parvum* and production of infectious oocysts

To determine whether the ALI culture system would support the growth of host-adapted IId subtypes of *C. parvum*, we infected ALI cultures with the virulent IId-HLJ ( $1 \times 10^5$  oocysts per Transwell). There was an ~300-fold amplification of IId-HLJ from the infection dose, which was higher than the ~70-fold amplification of Ila-Waterborne (Figures 1C and 2A). Both H&E and immunohistochemical (IHC) analyses showed a large number of parasites on the surface of the ALI monolayers (Figure 2B). Immunofluorescence microscopy using antibodies against cellular markers villin and Muc2 confirmed that the ALI treatment promoted cell differentiation (Figure 2C). The production of oocysts was supported by immunofluorescence microscopy using antibodies against oocysts (Figure 2D).

To assess the infectivity of oocysts generated, we infected IFN- $\gamma$  knockout (GKO) mice with parasites harvested from ALI cultures infected with sporozoites, after killing immature stages by bleach treatment of the harvested parasites (Figure 2E). Mice infected with DPI 1 material (containing no oocysts) showed no clinical signs of cryptosporidiosis. In contrast, mice infected with DPI 3 material (containing newly generated oocysts) showed inactivity, rough hair, arched back and sticky fecal pellets, starting at DPI 7. The oocyst shedding reached peak at DPI 10, with oocyst per gram (OPG) of feces values reaching  $\sim 10^8$  (Figure 2E). The IId subtype identity of parasites shed by mice was confirmed by *gp60* sequence analysis. Consistent with the oocyst shedding results, H&E-stained sections of intestinal tissues from mice infected with DPI 3 material showed the presence of high parasite burdens, while no parasites were seen in tissues from mice inoculated with DPI 1 material (Figure 2F).

We performed scanning (SEM) and transmission electron microscopy (TEM) to further examine the development of *C. parvum* in ALI cultures. SEM images of ALI cultures infected with IId-HLJ showed the presence of parasites on the surface of the monolayers in clusters (Figure 3A). Elongation and reduction in numbers of microvilli were seen in cells infected with the parasites (Figure 3A). Multiple life cycle stages

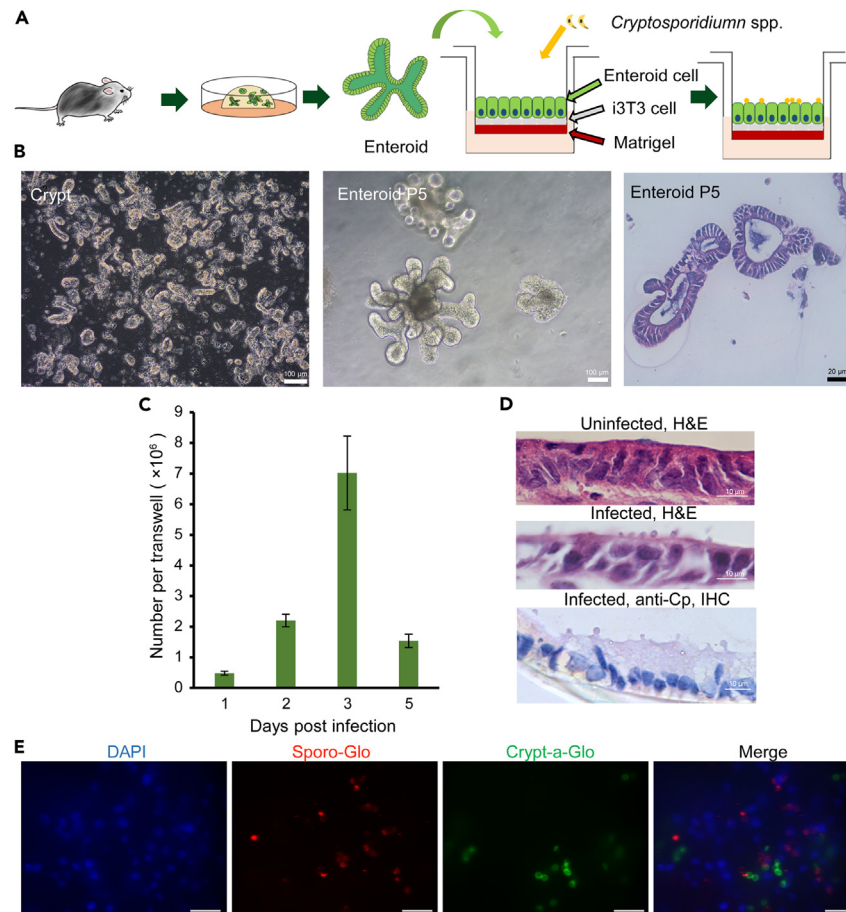


**Figure 1. Establishment of an enteroid-derived air-liquid interface (ALI) system for cultivation of *Cryptosporidium parvum* Ila-Waterborne isolate *in vitro***

(A) Schematic outline of the process of creating mouse intestinal organoid stocks and establishing the ALI system for infection.

(B) Images of murine intestinal crypts (left image), enteroid passage No. 5 (P5, middle image), and H&E-stained sections of P5 (right image). Crypts isolated from mouse intestines looked like pellets initially. After 3 days of cultivation, the enteroids formed with budding structures and an internal chamber.

(C) Propagation of the *C. parvum* Ila subtype in the ALI system ( $1 \times 10^5$  oocysts per Transwell) as measured by qPCR,  $n = 3$ . Means  $\pm$  SEM of three Transwells per timepoint from a representative experiment.

(D) Histological (H&E) and immunohistochemistry (IHC) microscopic images of the ALI system infected with *C. parvum* Ila-Waterborne oocysts at DPI 3. Developmental stages (globular structures) of *C. parvum* are visible on the surface of cells in infected ALI cultures. Scale bars, 10  $\mu$ m.

(E) Immunofluorescent microscopy of ALI monolayers infected with Ila-Waterborne sporozoites, showing the presence of developmental stages (stained with Sporo-Glo mAb) and oocysts (stained with Crypt-a-Glo mAb) at DPI 3. Scale bars, 20  $\mu$ m.

were observed under TEM, including meronts, macrogamonts and oocysts (Figure 3B). Sporulated oocysts surrounded by parasitophorous vacuole membrane (PVM) were recognized on the surface of some infected cells at DPI 3, confirming that the ALI system supported the full development of the *C. parvum* IId subtype (Figure 3B).

### The ALI system permitted accessible cryopreservation of *C. parvum*

To examine whether ALI cultures infected with *C. parvum* could be cryopreserved, we froze ALI cultures 6 h (ALI-6h) or 12 h (ALI-12h) after infection with sporozoites of IId-HLJ (Figure 4A). After storage in liquid nitrogen for over one month, the preserved cultures were thawed and seeded onto ALI cultures (Figure 4A). Results of the qPCR analysis showed that the numbers of recovered parasites from cryopreserved ALI-6h cultures increased between DPI 1 and 3 ( $p = 0.0421$ ), while the increase in parasite burden was much less obvious in ALI cultures inoculated with cryopreserved ALI-12h cultures ( $p = 0.8546$ ) (Figure 4B). Immunofluorescent examinations showed that both developing stages (stained with Sporo-Glo) and oocysts (stained with Crypt-a-Glo) were presented at DPI 3 in ALI cultures infected with recovered parasites (Figure 4C). H&E-stained sections showed that parasites were adhering in the top of ALI monolayers infected with recovered ALI-6h cultures, although we failed in detecting parasites on the surface of cultures infected with cryopreserved ALI-12h cultures, probably due to the lower infection intensity (Figure S1A). This was confirmed by the results of the IHC analysis of cultures (Figure S1A).

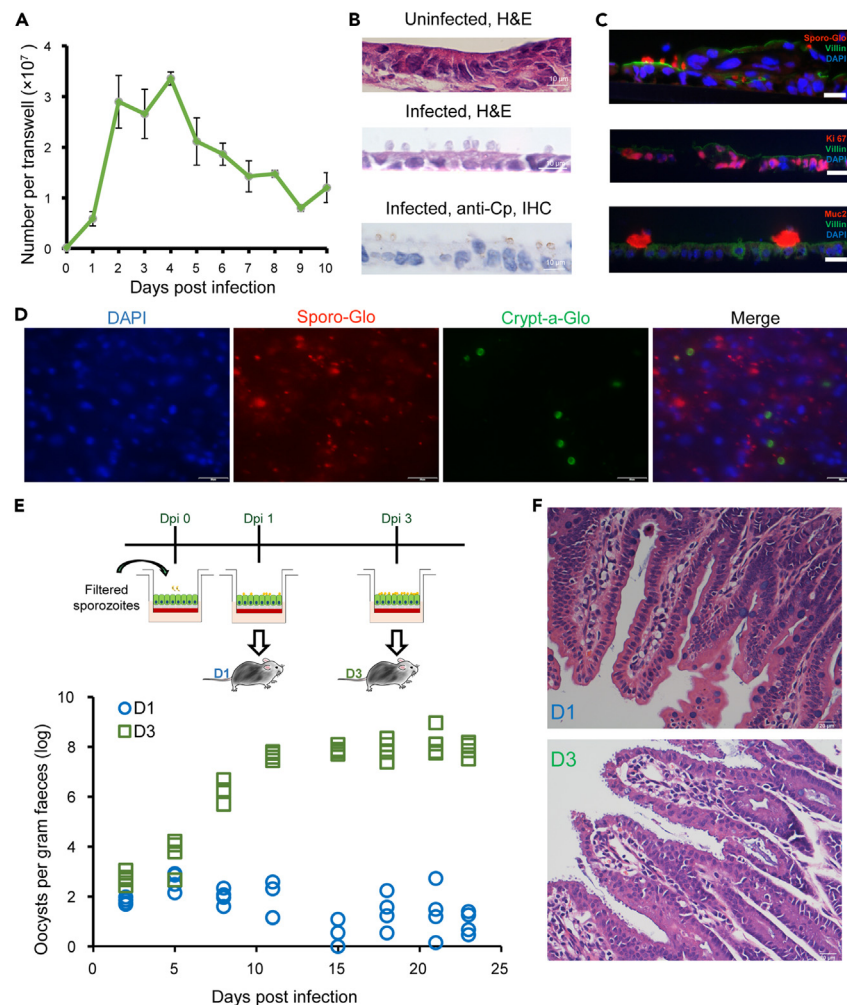


**Figure 2. Complete development of the IId subtype of *Cryptosporidium parvum* in the murine organoid-derived air-liquid interface (ALI) system**

(A) Proliferation of IId-HLJ isolate cultured in the ALI system ( $1 \times 10^5$  oocysts per Transwell) as measured by qPCR,  $n = 3$ . Means  $\pm$  SEM of three Transwells per timepoint from a representative experiment.

(B) Images of ALI sections stained with H&E or rabbit antibodies against *C. parvum* using immunohistochemistry (IHC), DPI 3. Developmental stages of *C. parvum* are visible on the surface of cells in infected ALI cultures. Scale bars, 10  $\mu$ m.

(C) Immunofluorescence images of the sections of the ALI cultures infected with IId-HLJ at DPI 3 using antibodies against Ki-67 (a marker for replicating cells), Muc2 (a marker for goblet cells) and Sporozo-Glo (reactive with intracellular stages of *C. parvum*). Scale bars, 10  $\mu$ m.

(D) Immunofluorescent microscopic images of the ALI cultures infected with IId-HLJ sporozoites after staining with Sporozo-Glo (reactive with developing stages) and Crypt-a-Glo (reactive with oocysts) antibodies against *C. parvum*, DPI 3. Scale bars, 20  $\mu$ m.

(E) Patterns of oocyst shedding in mice ( $n = 4$ ) orally gavaged with ALI cultures that were infected with IId-HLJ sporozoites for 1 (D1) and 3 (D3) days. The cultures were treated with 10% bleach to kill immature stages prior to mouse inoculation.

(F) Images of H&E-stained sections of the small intestine from these mice at DPI 23. Developmental stages of *C. parvum* are visible only on the surface of the ileum from mice infected with D3 cultures. Scale bars, 20  $\mu$ m.

To assess if ALI infection with routine HCT-8 cultures of *C. parvum* would allow the cryopreservation of the pathogen, we performed ALI infection studies with cryopreserved HCT-8 cells that were infected with sporozoites of the IId subtype of *C. parvum* for 6 h (HCT-6h). The thawed HCT-6h cultures were seeded onto ALI cultures, with the parasite growth being determined by qPCR and immunofluorescent analysis (Figure 4D). The parasite load in ALI cultured infected with cryopreserved *C. parvum* in HCT-6h increased  $\sim 2$ -fold between DPI 1 and DPI 3 ( $p = 0.0041$ ) (Figure 4E). Both developing stages and oocysts were seen at DPI 3 in ALI cultures (Figure 4F). Developing stages were also observed on the surface of ALI cultures infected with HCT-6h under H&E and IHC microscopy (Figure S1B).

To determine if the oocysts collected from ALI cultures infected with cryopreserved *C. parvum* were viable and infectious, we inoculated GKO mice with the ALI cultures described above. Cryopreserved ALI-6h or HCT-6h were cultured further in ALI system for 4 days to produce oocysts. Mice inoculated with bleach-treated ALI materials started to shed oocysts at  $\sim$  DPI 6, with peak oocyst shedding of  $\sim 10^8$  OPG at DPI

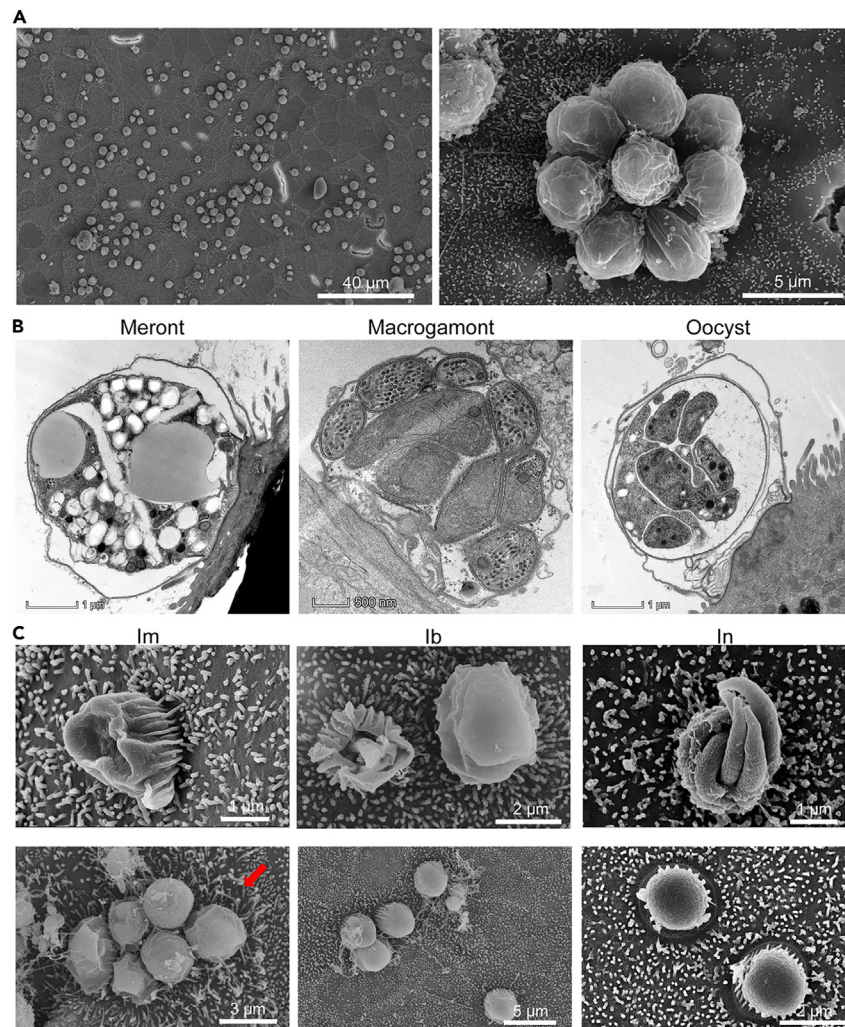


**Figure 3. Scanning (SEM) and transmission electron microscopy (TEM) images of developmental stages of *Cryptosporidium* spp. in the enteroid-derived air-liquid interface (ALI) system**

(A) SEM images showing the development of *C. parvum* IId-HLJ isolate on top of the ALI monolayers. The left image shows the elongation and reduction in numbers of microvilli on infected cells, while the right image shows a cluster of parasites developed from eight merozoites released from one mature meront. (B) TEM images of one meront, macrogamont and oocyst each of *C. parvum* within the parasitophorous vacuole on the apical surface of ALI monolayers. The ALI cultures were infected with  $3 \times 10^5$  sporozoites per Transwell.

(C) SEM images of *C. hominis* developed in ALI cultures for three days. The ALI monolayers were infected with Ib, Im and In isolates. Elongation and reduction in numbers of microvilli are visible near the developing parasites in the lower left image (indicated by a red arrow).

12 (Figures 4G and 4H). Subtyping of the parasites by sequence analysis of the *gp60* gene confirmed that the oocysts inoculated and produced after infection were identical. Microscopy of H&E-stained sections of the ileum from mice infected with HCT-6h or ALI-6h material showed heavy *C. parvum* infection (Figure S1C).

In the present study, we used only frozen cultures that had been stored for one month. Future studies should evaluate the impact of longer storage on the revival of cryopreserved parasites.

### The ALI system supported complete development of multiple *C. hominis* isolates

To assess the infectivity of *C. hominis* isolates to murine enteroids, we infected ALI cultures with  $1 \times 10^5$  oocysts (Figures 5A and 5B) or  $4 \times 10^5$  sporozoites (Figures 5C and 5D) per Transwell. The three genetically unique *C. hominis* subtypes from macaque monkeys were used, including Ib, In and Im. They showed a similar infection pattern in ALI cultures, with the parasite burden peaking at DPI 3 (Figure 5A). Among them, Ib and In generated peak parasite burden of over  $1.5 \times 10^7$  parasites per Transwell, while Im generated peak parasite burden of  $4 \times 10^6$  (Figure 5A). For all three *C. hominis* isolates, the number of parasites per Transwell at DPI 3 was significantly higher than that at DPI 1 (Ib,  $p = 0.0047$ ; In,  $p = 0.0130$ ; Im,  $p = 0.0513$ ) (Figure 5A).

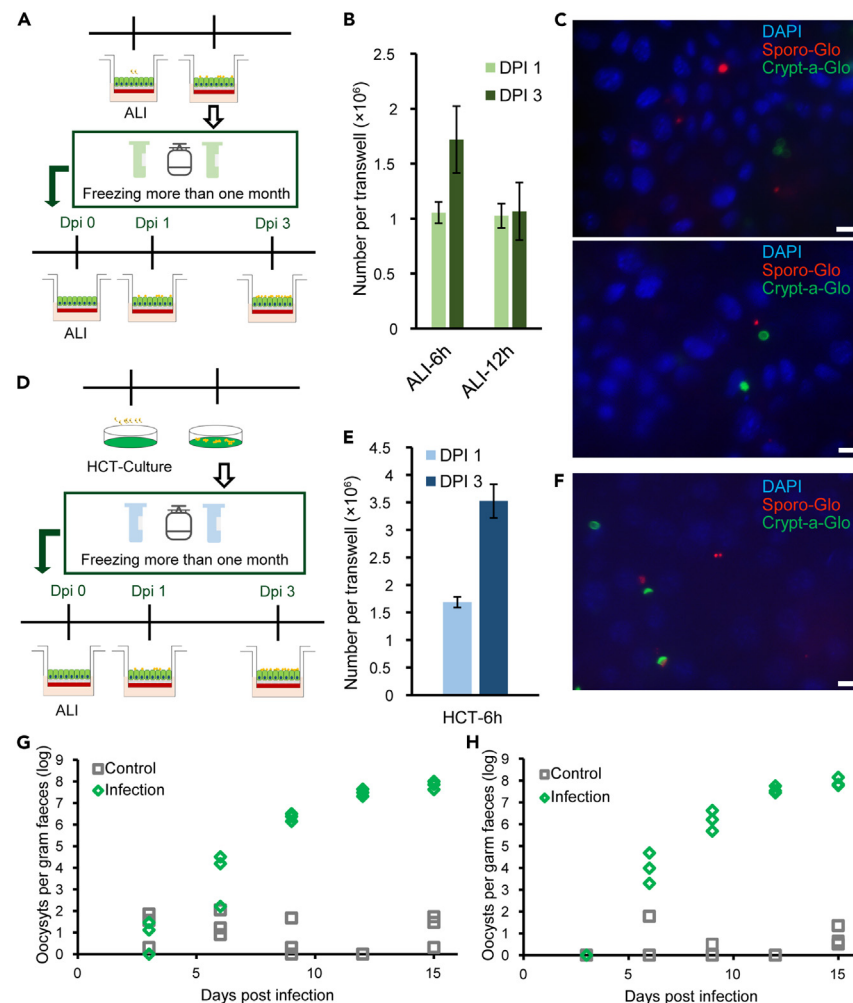


**Figure 4. An accessible cryopreservation method of *Cryptosporidium parvum* using the air-liquid interface (ALI) system**

(A) Schematic outline of the process of the cryopreservation of *C. parvum* using the ALI system. *C. parvum* IId-HLJ was cultured in ALI for 6 (ALI-6h) or 12 h (ALI-12h). The infected ALI cells were cryopreserved in liquid nitrogen for over one month prior to be inoculated into new ALI cultures for recovery and continued cultivation of *C. parvum* for one or three more days.

(B) Proliferation of the recovered parasites in ALI cultures at DPI 1 and DPI 3,  $n = 3$ . New ALI cultures were infected with cryopreserved ALI-6h or ALI-12h. Means  $\pm$  SEM of three Transwells per timepoint from a representative experiment.

(C) Immunofluorescence images of the ALI monolayers infected with ALI-6h or ALI-12h for three days, showing the presence of developing stages (reactive to Sporo-Glo antibodies) and oocysts (reactive to Crypt-a-Glo antibodies). Scale bars, 10  $\mu$ m.

(D) Schematic outline of the process of the cryopreservation of *C. parvum* using inoculation of ALI cultures with parasites cultured in HCT-8 cells. New ALI cultures were infected with cryopreserved HCT-8 cells 6 h after they were infected with IId-HLJ (HCT-6h).

(E) Proliferation of recovered parasites in ALI cultures one and three days after they were inoculated with cryopreserved HCT-6h,  $n = 3$ . Means  $\pm$  SEM of three Transwells per timepoint from a representative experiment.

(F) Immunofluorescence image of the ALI monolayers infected with HCT-6h for three days. Scale bars, 10  $\mu$ m.

(G and H) Patterns of *Cryptosporidium* oocyst shedding in mice. Infection: mice were orally gavaged with the ALI materials infected with ALI-6h (G) or HCT-6h (H) for four days; Control: mice were orally gavaged with PBS.

H&E microscopy revealed the presence of numerous parasites on the surface of the ALI monolayers (Figure 5B). Immunofluorescence microscopy of the ALI cultures infected with sporozoites showed the presence of both developing stages (reactive to Sporo-Glo antibodies) and mature oocysts (reactive to Crypt-a-Glo antibodies) (Figure 5C). SEM analysis of the ALI monolayers identified the presence of parasites on the surface of many cells, with apparent elongation of microvilli near the parasites (Figure 3C).

To determine whether the *C. hominis* oocysts produced in ALI cultures were viable and infectious, we infected mice with ALI cultures that were infected with filtered  $5 \times 10^5$  Ib sporozoites per Transwell and harvested at DPI 1 or DPI 3. Mice infected with DPI 3 materials started shedding oocysts at DPI 6 and reached peak at DPI 15 with OPG values of  $\sim 10^8$ , while mice infected with DPI 1 material remained uninfected (Figure 5D). The Ib subtype identity of parasites shed by mice was confirmed by *gp60* sequence analysis. Microscopy of H&E-stained sections

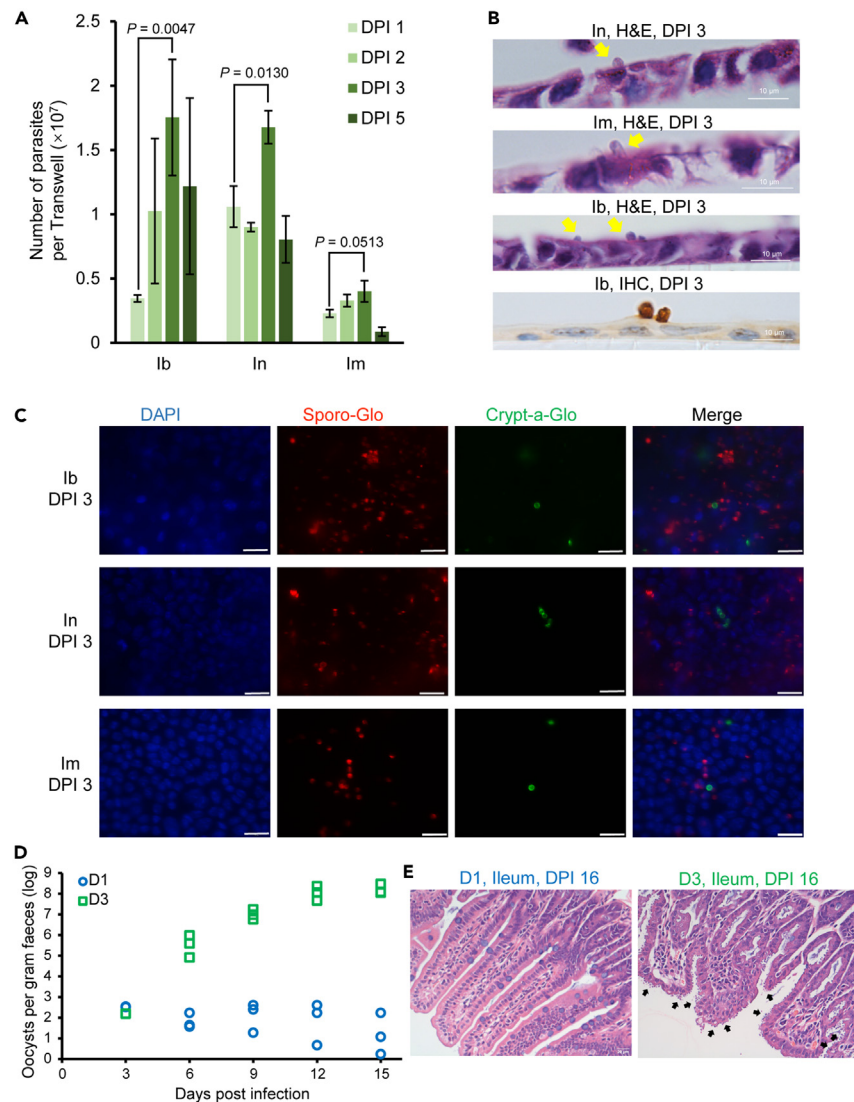


**Figure 5. Cultivation of *Cryptosporidium hominis* using the enteroid-based air-liquid interface (ALI) system**

(A) Growth of lb, lm, and ln subtypes of *C. hominis* in ALI after infection with  $1 \times 10^5$  oocysts/Transwell,  $n = 3$ . Means  $\pm$  SEM of three Transwells per timepoint from a representative experiment. Data were analyzed using a 2-tailed unpaired Student's t test.

(B) H&E microscopy images of ALI monolayers infected with lb, lm and ln, showing the presence of parasites (marked with arrows) on the surface of epithelial cells.

(C) Immunofluorescence images of ALI cultures infected with  $4 \times 10^5$  sporozoites of three *C. hominis* subtypes, showing the presence of developmental stages (reactive to Sporoglo antibodies) and oocysts (reactive to Crypt-a-Glo antibodies). Scale bars, 20  $\mu$ m.

(D) Patterns of oocyst shedding in mice ( $n = 4$ ) orally gavaged with ALI materials that were infected with sporozoites of *C. hominis* lb subtype for one (D1) and three days (D3).

(E) Images of H&E-stained sections of the ileum of mice infected with D1 or D3 materials described above for 16 days. Scale bars, 20  $\mu$ m.

of the ileum from mice infected with DPI 3 cultures showed numerous parasites on the surface of intestinal epithelial cells, while those inoculated with DPI 1 culture remained uninfected (Figure 5E).

### Transcriptomic responses induced by *C. hominis* differed significantly between ALI and HCT-8 cultures

To characterize host cell responses to *C. hominis* infection *in vitro*, we analyzed the transcriptomes of ALI and HCT-8 cultures infected with the lb subtype of *C. hominis* at DPI 3. Principal component analysis (PCA) showed significant differences in host gene expression between the infected and control groups in both ALI and HCT-8 cultures (Figure 6A). A total of 4141 differentially expressed genes (DEGs) were identified in murine enteroids infected with *C. hominis* at DPI 3, with 2328 up- and 1813 down-regulated genes, while 2141 DEGs were identified in HCT-8 cultures with 701 up- and 1440 down-regulated genes (Figure 6B).

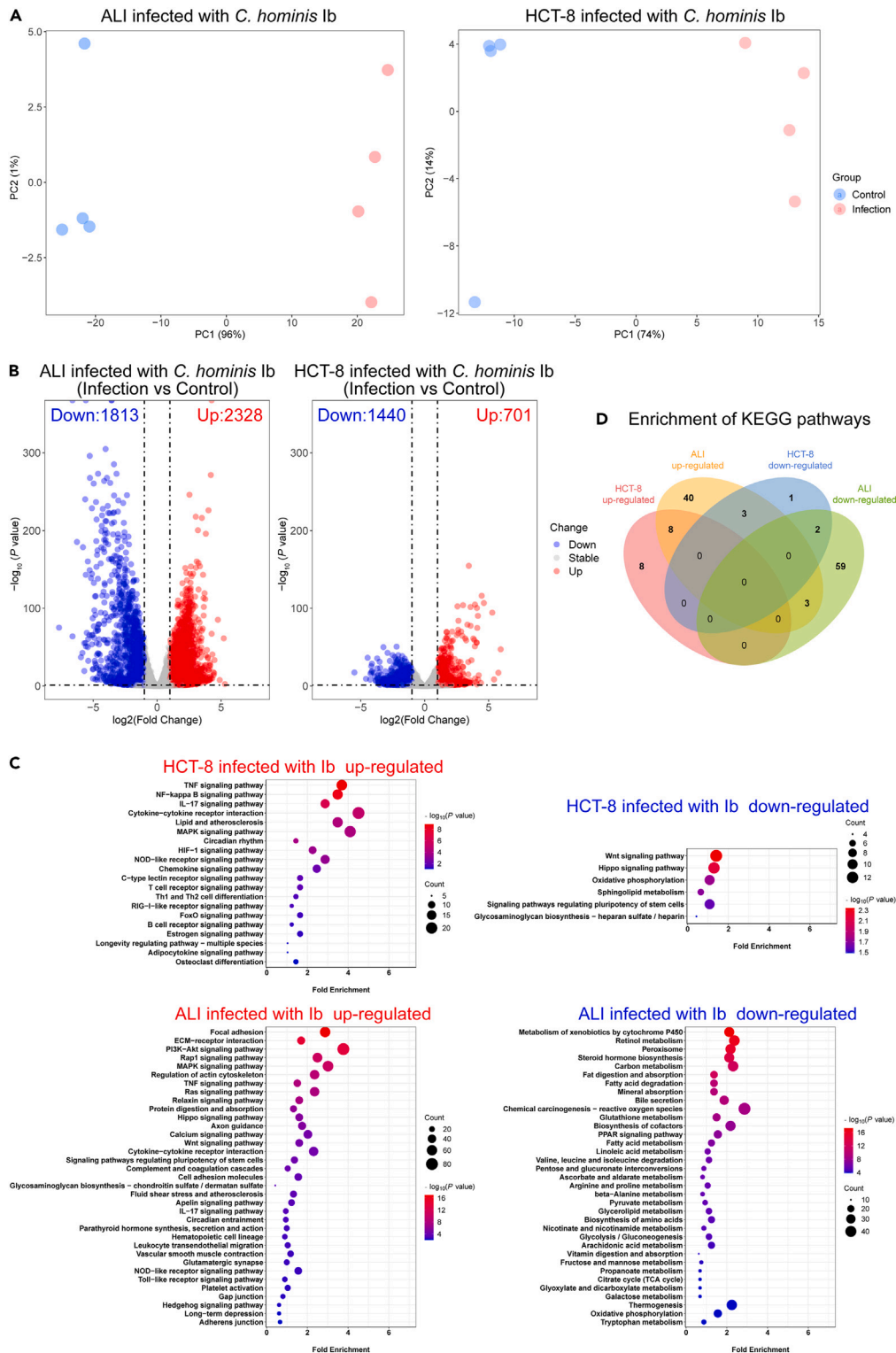


**Figure 6. Transcriptomic responses of host genes in air-liquid interface (ALI) monolayers and HCT-8 cells after infection with *Cryptosporidium hominis*** (A) Differences in transcriptomic responses between control ALI or HCT-8 cultures and those infected with the *C. hominis* Ib subtype for 3 days, as indicated by principal component analysis of the RNA-seq data, n = 4. (B) Volcano plots showing numbers of differentially expressed genes (DEGs) between control and infected ALI or HCT-8 cultures.

**Figure 6. Continued**

(C) Kyoto Encyclopedia of Genes and Genomes (KEGG) analysis of DEGs of ALI or HCT-8 cultures after infection with Ib. The y axis shows significantly enriched KEGG pathways while the x axis indicates the fold enrichment of DEGs.

(D) Venn diagram of shared and unique KEGG pathways between ALI and HCT-8 cultures infected with Ib.

The up-regulated transcripts in the HCT-8 cells infected with Ib were significantly enriched for immune responses such as TNF, NF- $\kappa$ B, IL-17 and MAPK signaling pathways and NOD-like, TOLL-like and RIG-I-like receptor signaling pathways. The down-regulated DEGs involved seven pathways, including the Wnt and Hippo signaling pathways, metabolic pathways, oxidative phosphorylation, sphingolipid metabolism, pluripotency of stem cells, and glycosaminoglycan biosynthesis (Figure 6C). In GO analysis of the RNA-seq data, the up-regulated genes were mainly involved in inflammatory and cell development processes, while the down-regulated DEGs were mainly involved in cell cycle (Figure S2).

Compared with those in HCT-8 cells, transcriptional responses in ALI cultures infected with Ib were much more robust (Figure 6D). Among the up-regulated DEGs in ALI cultures, most of them involved immune (including PI3K-Akt, Wnt, Ras, MAPK, TNF, and IL-17 signaling pathways and NOD-like and TOLL-like receptor signaling pathways) and inflammatory (including complement and coagulation cascades, leukocyte migration, vascular contraction and platelet activation) responses and cell adhesion and junction (including focal adhesion, ECM-receptor interaction, axon guidance, cell adhesion molecules, gap junction and adherens junction) (Figure 6C). In contrast, the down-regulated DEGs were mainly involved in absorption, biosynthesis and metabolism of various nutrients (Figure 6C). This was also supported by GO analysis of the DEGs (Figure S2).

Among the 99 KEGG pathways uniquely enriched in ALI cultures, 40 pathways were up-regulated and 59 down-regulated (Table S1). In contrast, only 9 pathways were uniquely enriched in HCT-8 cells infected with Ib (including 8 up- and 1 down-regulated pathways) (Table S1). Most of the uniquely upregulated pathways in Ib-infected ALI cultures and HCT-8 cells involved immune and inflammatory responses, while the downregulated pathways mainly involved nutrient biosynthesis. Cell adhesion and junction and metabolism were uniquely enriched among the up- or downregulated DEGs in ALI cultures, indicating that these cell responses were associated with the lack of further development of the parasites in HCT-8 cells. Of particular interest is the expression of the Wnt and Hippo signaling pathways, which were down-regulated in HCT-8 cultures but up-regulated in ALI cultures after *C. hominis* infection (Table S1).

**Comparative transcriptomic analysis revealed major differences in the expression of *C. hominis* genes between ALI and HCT-8 cultures**

In addition, we compared the transcriptomic responses of *C. hominis* genes in HCT-8 and ALI cultures (Figure 7A; Table S2). Among the 3913 protein-encoding genes in the *C. hominis* genomes, 1827 were expressed in both ALI and HCT-8 cultures. An additional 2005 genes had expression in ALI cultures (Figure 7B; Table S2). Among the top 200 highly expressed genes in ALI cultures, 55 had low expression in HCT-8 cultures ( $\log_2\text{FPKM} < 4.0$ ). Most of them were genes encoding ribosomal proteins and *Cryptosporidium*-specific hypothetical proteins, which are required for parasites growth and proliferation. This suggests the occurrence of developmental arrest of *C. hominis* in HCT-8 cultures at 72 h (Figure 7B; Table S2). In contrast, the KEGG analysis of the 2005 *C. hominis* genes uniquely expressed in ALI cultures had shown significant enrichment for metabolism and biosynthesis, homologous recombination and meiosis, proteolysis, and RNA degradation (Figure S3). In particular, the expression of genes encoding oocyst wall and crystalloid body proteins was higher in Ib-infected ALI cultures than Ib-infected HCT-8 cultures (Figure 7C). As these genes are preferentially expressed in the macrogamonts, zygotes and oocysts,<sup>13,23,24</sup> these data support the generation of oocysts in ALI cultures but not in HCT-8 cultures.

**DISCUSSION**

In this report, we have described procedures for the generation of murine enteroids and refined the procedures for the maintenance of the ALI culture system. The modified ALI system allows the completion of the entire life cycle of *C. parvum* and *C. hominis* and propagation of isolates, producing infectious oocysts within three days. As the ALI system could be infected with frozen *C. parvum* cultures, it provides an accessible cryopreservation of *Cryptosporidium* spp. for long-term storage. RNA-seq analyses of the ALI and HCT-8 cultures infected with *C. hominis* showed significant differences in the transcriptome profiles of both the host cells and parasites, providing important information on host-parasite interactions.

The procedures of murine enteroid generation and differentiation described here allow routine cultivation of *Cryptosporidium* spp. While 3D culture systems have allowed the completion of the full life cycle of *C. parvum* in HCT-8 cells,<sup>25,26</sup> the newly established ALI system of *C. parvum* has the advantage of mimicking the native intestinal environment by having diverse populations of intestinal cells in cultures.<sup>18</sup> In the present study, we have refined the operational procedures for isolation of intestinal crypts and cultivation of enteroids by modifying the treatment of i3T3 cells, culture medium, and digestion method of enteroids. In particular, the replacement of irradiation of i3T3 cells with mitomycin C treatment makes the generation and cultivation of enteroids more adaptable to most laboratories.

The modified ALI system can be adapted for *in vitro* studies of diverse *C. parvum* isolates. In the present study, we have used it effectively in the cultivation of one *C. parvum* IId isolate. Prior to this, *in vitro* studies of *C. parvum* were done exclusively with IIa subtypes.<sup>17,18,25,26</sup> Although IIa and IId subtypes differ from each other in distribution and host ranges,<sup>8</sup> we have poor understanding of the determinants of these biological differences. In the present study, we have used the ALI system effectively in the cultivation of the virulent IIdA20G1-HLJ isolate. The oocysts generated by the enteroids were infective to mice. In fact, the IId isolate generated much higher parasite loads in ALI

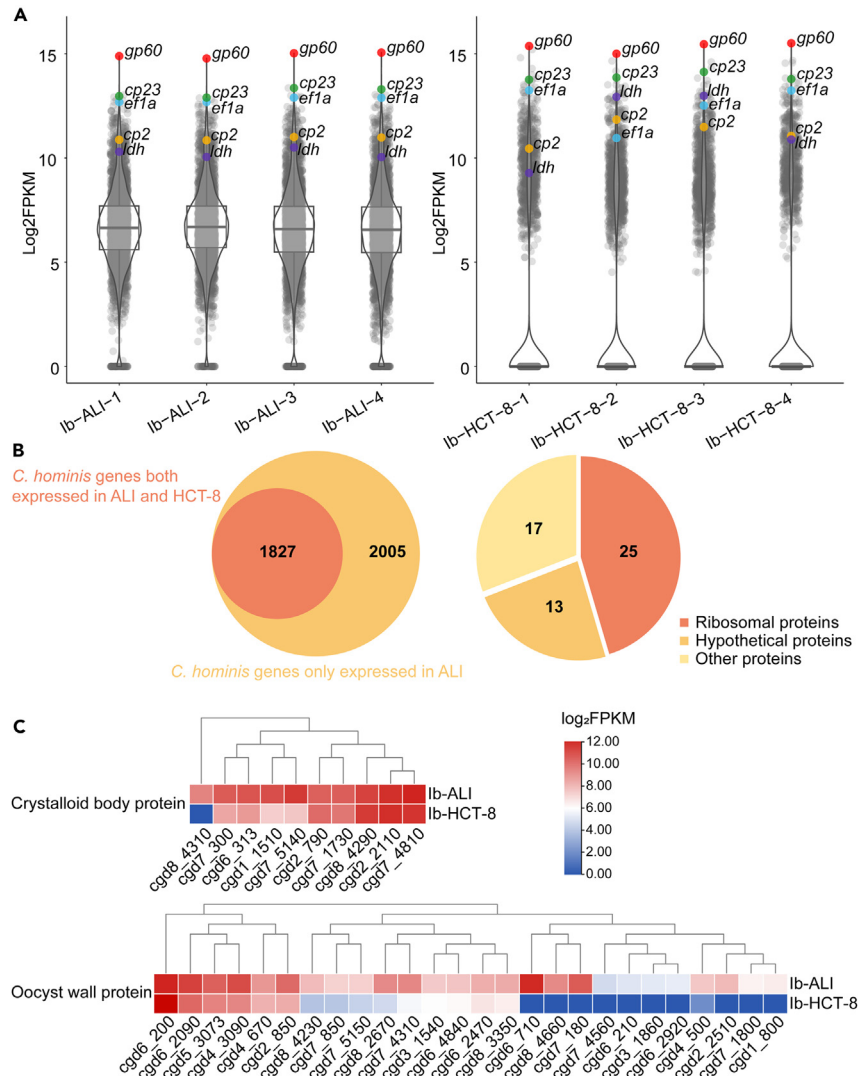


**Figure 7. Profiles of the expression of *Cryptosporidium hominis* genes in the enteroid-based air-liquid interface (ALI) and HCT-8 cultures**

(A) Violin plots of the expression profiles of *C. hominis* genes in lb-infected ALI or HCT-8 cultures for 3 days, n = 4 for each group.

(B) Venn diagram (the left figure) showing the shared (orange part) and unique genes (yellow part) of *C. hominis* lb subtype in ALI cultures in comparison with in HCT-8 cells; pie chart (the right figure) showing the category of the 55 most differentially expressed genes (DEGs) of *C. hominis* in ALI cultures and in HCT-8 cells. The 55 genes had low expression in HCT-8 cultures (log<sub>2</sub>FPKM < 4.0), but were among the top 200 highly expressed *C. hominis* genes in ALI cultures.

(C) Heat maps of the expression profiles of the genes encoding oocyst wall proteins (preferentially expressed in macrogamonts, zygotes and oocysts) and crystalloid body proteins (preferentially expressed in sporozoites) of *C. hominis* lb subtype in ALI cultures and HCT-8 cells.

cultures than the reference IlaA17G2R1-Waterborne isolate. This is in agreement with the result of comparisons of the infectivity and virulence of the two isolates in GKO mice.<sup>27</sup> Therefore, the Ild-HLJ isolate was used in subsequent studies, including those on the cryopreservation of *C. parvum*. However, there could be intrinsic differences in culture characteristics among *C. parvum* isolates. IldA20G1-HLJ oocysts produced in ALI cultures appear to be unable to excyst spontaneously, therefore failed in continuously infecting enteroids. This is different from previous findings obtained using a Ila isolate.<sup>18</sup>

More importantly, we have demonstrated that *C. hominis* Im, lb, and ln subtypes can be cultivated *in vitro* using the ALI system. *C. hominis* is a primate-adapted species and a major cause of human cryptosporidiosis worldwide.<sup>4</sup> The three *C. hominis* isolates we used were from crab-eating macaques in China, but have more subtelomeric genes than the common *C. hominis* subtype families (Ia, Ib, Id, Ie, and If) in humans. Because these subtelomeric genes have been associated with broad host range of *C. parvum*,<sup>7,28</sup> the three isolates could have broader host range than regular *C. hominis* isolates. This is probably the reason for the high infectivity of the three *C. hominis* isolates to GKO mice. Therefore, taking advantage of their mouse infectivity, we have been able to adopt the murine ALI system for the cultivation of *C. hominis*. Here we have demonstrated the complete development of three *C. hominis* isolates *in vitro*, producing oocysts that are infective to GKO

mice. Among the three *C. hominis* subtype families we used in this study, Ib and In generated higher infectivity and oocyst output than Im, reaffirming the utility of the ALI system in comparative studies of diverse *Cryptosporidium* isolates *in vitro*. The growth patterns of these three *C. hominis* subtypes in ALI cultures agree with their infectivity and virulence in GKO mice.<sup>29</sup>

The ALI-*C. hominis* infection model provides a good mechanism to study the host-parasite interactions *in vitro*. Recently, Greigert et al. demonstrated that the ALI platform supports the complete development of one human *C. hominis* isolate. This valuable study focuses on the transcriptomic changes of the host infected with *C. hominis* after 24 h, and shows that *Cryptosporidium* infection induces a strong interferon response in host cells and reduces rotavirus infectivity during co-infection of the two pathogens.<sup>19</sup> Here we performed RNA-seq in ALI and HCT-8 cultures after *C. hominis* Ib infection for 72 h. Therefore, the two studies targeted different *Cryptosporidium* stages: sexual stages and oocysts are present in ALI cultures after 72 h of infection, whereas only asexual stages are present in ALI cultures at 24 h, and HCT-8 cultures support only partial pathogen development without oocyst production. Our data of the RNA-seq analysis of ALI cultures indicate that *C. hominis* infection upregulates various signaling pathways associated with immune and inflammatory responses. The intensity and nature of these host cell responses differ significantly from those induced by *C. hominis* infection of HCT-8 cells. This is expected, as the latter consists of one single type of adenocarcinoma cells of the colon compared with diverse populations of intestinal cells of the enteroids. The host cell responses detected in *C. hominis*-infected ALI cultures, however, are similar to those seen recently in *C. parvum* and *C. tyzzeri*-infected ileum.<sup>30</sup>

Interestingly, the transcriptomic profiling of host cell responses has shown significant downregulation of various metabolic pathways in *C. hominis*-infected ALI cultures, including both nutrient digestion, absorption and biosynthesis. Although cryptosporidiosis is well known for causing malnutrition in children, the mechanism for this is not clear.<sup>31</sup> The data generated here indicate that *Cryptosporidium* spp. could cause malnutrition by inhibiting host metabolism in addition to affecting nutrient absorption. This agrees with the observation in the present study of reduced number and elongation of microvilli on the epithelial cells infected with *Cryptosporidium* spp., which was previously observed in *C. parvum*-infected HCT-8 cells.<sup>32</sup> Transcriptomic studies of *C. parvum*-infected HCT-8 cultures, however, have failed to show downregulated nutrient absorption and metabolism in host cells,<sup>33</sup> reaffirming the conclusion that the ALI system is much better than the HCT-8 system for studying cryptosporidiosis-associated host cell responses.

The RNA-seq analysis has further shown significant differences in the expression of *C. hominis* genes between ALI and HCT-8 cultures, with the former having a significantly higher expression of genes encoding proteins associated with oocysts (such as oocyst wall proteins) and sporozoites (such as crystalloid body proteins).<sup>23</sup> Although many genes encoding oocyst wall proteins and crystalloid body proteins have been identified in late developmental stages, we still have a rudimentary understanding of the sexual stages of *Cryptosporidium* spp. Parasite DEGs between ALI cultures and HCT-8 cells are potential candidate genes involved in the fertilization process of *Cryptosporidium* spp. (Figure 7C). These data provide further evidence for complete development of *C. parvum* and *C. hominis* in ALI cultures.

The new ALI system can also be used in cryopreservation of *Cryptosporidium* spp. Reliable cryopreservation of *Cryptosporidium* oocysts has been a long-standing challenge. Recently, methods have been developed for cryopreservation of *C. parvum* and *C. hominis* by freezing permeabilized oocysts.<sup>20–22</sup> These cryopreservation methods cryopreserve oocysts by vitrification using special containers, such as silica microcapillaries or specially designed sample vitrification cassettes. However, the volume of silica microcapillaries (2  $\mu$ L) is limited and the specially designed vitrification cassettes are inaccessible in most laboratories. These oocyst cryopreservation methods have not been widely used because of these limitations. In addition, frozen storage of intracellular stages of *Cryptosporidium* spp. has been tried previously.<sup>34–37</sup> Paziewska-Harris et al. demonstrated that *C. parvum* could be recovered from infected cells after 6 and 12 months of storage in liquid nitrogen, with the number of recovered parasites increasing in HCT-8 cultures.<sup>37</sup> However, the recovered parasites are unlikely to develop into oocysts, because it is well established that HCT-8 and other cell lines only support the development of *C. parvum* into sexual stages.<sup>13</sup> Taking advantage of the ability by *C. parvum* to complete full life cycle and producing infectious oocysts in the enteroid-based ALI cultures, we have developed a novel cryopreservation method by freezing young intracellular parasites cultured in ALI or HCT-8 cultures and recovering them through further cultivation in ALI monolayers. This allows the recovered parasites to complete their development after the cryopreservation. To reduce the cost of time and labor, we amended the protocol by using HCT-8 cultures to support the growth of parasites to trophozoites before freezing. This is expected to make no difference because *C. parvum* develops equally well in both HCT-8 cells or ALI cultures during the early cultivation period. Although the new cryopreservation method allows accessible storage of *Cryptosporidium* in liquid nitrogen for at least one month, long-term storage of *Cryptosporidium* remains to be tested.

We think the cryopreservation of trophozoites soon after the invasion of *C. parvum* is key to the success of this new approach, allowing further replication of the parasites in ALI cultures after inoculation of the cryopreserved materials. We have tried to freeze cells infected with parasites for 24 h or 48 h in preliminary experiments, but did not observe any oocysts in the ALI cultures inoculated with the recovered cells using IFA. In contrast, as shown in the study, the cryopreserved cell cultures containing early stages (ALI/HCT-6h and ALI-12h) both induced the generation of oocyst after their revival in ALI cultures. We also observed that the growth of recovered parasites of ALI-6h was higher than that of ALI-12h in ALI cultures (Figure 4B). Because *C. parvum* in ALI-6h cultures were mostly trophozoites, we speculate that the revived trophozoites have the advantage of more rounds of asexual replication than merozoites and other stages in later cultures. Therefore, we used ALI-6h instead of ALI-12h for mouse infection.

In conclusion, the newly established enteroid system has been adapted effectively for the cultivation of host-adapted *C. parvum* and *C. hominis*, producing oocysts that are infective to mice. This allows not only comparative studies of the biology of the two major human pathogens but also cryopreservation of isolates. The use of the system in transcriptomic studies of *C. hominis* has provided preliminary evidence implicating the downregulations of host metabolism in the induction of malnutrition by cryptosporidiosis, and data on candidate genes potentially involved in the regulation of sexual reproduction and oocyst development.

## STAR★METHODS

Detailed methods are provided in the online version of this paper and include the following:

- KEY RESOURCES TABLE
- RESOURCE AVAILABILITY
  - Lead contact
  - Materials availability
  - Data and code availability
- EXPERIMENTAL MODEL AND STUDY PARTICIPANT DETAILS
  - *Cryptosporidium* isolates
  - Mice
- METHOD DETAILS
  - Establishment and maintenance of enteroids
  - Generation of ALI culture system and infection with *Cryptosporidium* spp
  - Cryopreservation of *C. parvum*-infected ALI or HCT-8 cultures
  - Measurement of *Cryptosporidium* growth
  - Microscopic analyses of ALI cultures
  - Experimental infection of GKO mice with cultured parasites
  - RNA-seq analysis of *C. hominis*-infected ALI and HCT-8 cultures
- QUANTIFICATION AND STATISTICAL ANALYSIS

## SUPPLEMENTAL INFORMATION

Supplemental information can be found online at <https://doi.org/10.1016/j.isci.2024.109563>.

## ACKNOWLEDGMENTS

This study was funded by National Natural Science Foundation of China (32030109 and U21A20258), Double First-Class Discipline Promotion Project (2023B10564003), and 111 Project (D20008). We thank Yingxin Liang for assistance in the generation of murine enteroids, Ruilian Jia, Ni Huang, Xuehua Chen, Haoyu Chen and Huimin Liu for provision of laboratory mice, and staff at the South China Agricultural University microscopy core facility for assistance with electron microscopy.

## AUTHOR CONTRIBUTIONS

L.X. and M.D. conceived and designed the study. L.X., Y.F., and Y.G. supervised the study. M.D. performed most of the experiments and data analysis. T.H. helped with the bioinformatics analysis. J.Z. and Y.W. helped with some experimental performance. F.Y. performed the ultra-structural analysis. Y.T. and W.Z. purified oocysts of *Cryptosporidium* isolates. W.H. and N.L. provided critical comments and contributed to study design. M.D. and L.C. wrote the manuscript and created the figures with input from all authors.

## DECLARATION OF INTERESTS

The authors declare no competing interests.

Received: January 5, 2024

Revised: February 21, 2024

Accepted: March 22, 2024

Published: March 26, 2024

## REFERENCES

1. Kotloff, K.L., Nataro, J.P., Blackwelder, W.C., Nasrin, D., Farag, T.H., Panchalingam, S., Wu, Y., Sow, S.O., Sur, D., Breiman, R.F., et al. (2013). Burden and aetiology of diarrhoeal disease in infants and young children in developing countries (the Global Enteric Multicenter Study, GEMS): a prospective, case-control study. *Lancet* **382**, 209–222.
2. Checkley, W., White, A.C., Jaganath, D., Arrowood, M.J., Chalmers, R.M., Chen, X.-M., Fayer, R., Griffiths, J.K., Guerrant, R.L., Hedstrom, L., et al. (2015). A review of the global burden, novel diagnostics, therapeutics, and vaccine targets for *Cryptosporidium*. *Lancet Infect. Dis.* **15**, 85–94.
3. Ryan, U., Zahedi, A., Feng, Y., and Xiao, L. (2021). An update on zoonotic *Cryptosporidium* species and genotypes in humans. *Animals* **11**, 3307.
4. Feng, Y., Ryan, U.M., and Xiao, L. (2018). Genetic diversity and population structure of *Cryptosporidium*. *Trends Parasitol.* **34**, 997–1011.
5. Nader, J.L., Mathers, T.C., Ward, B.J., Pachebat, J.A., Swain, M.T., Robinson, G., Chalmers, R.M., Hunter, P.R., van Oosterhout, C., and Tyler, K.M. (2019). Evolutionary genomics of anthroponosis in *Cryptosporidium*. *Nat. Microbiol.* **4**, 826–836.
6. Cama, V.A., Bern, C., Roberts, J., Cabrera, L., Sterling, C.R., Ortega, Y., Gilman, R.H., and Xiao, L. (2008). *Cryptosporidium* species and subtypes and clinical manifestations in children, Peru. *Emerg. Infect. Dis.* **14**, 1567–1574.
7. Guo, Y., Tang, K., Rowe, L.A., Li, N., Roellig, D.M., Knipe, K., Frace, M., Yang, C., Feng, Y., and Xiao, L. (2015). Comparative genomic analysis reveals occurrence of genetic recombination in virulent *Cryptosporidium hominis* subtypes and telomeric gene

- duplications in *Cryptosporidium parvum*. *BMC Genom.* 16, 320.
8. Guo, Y., Ryan, U., Feng, Y., and Xiao, L. (2022). Emergence of zoonotic *Cryptosporidium parvum* in China. *Trends Parasitol.* 38, 335–343.
  9. Bhalchandra, S., Cardenas, D., and Ward, H.D. (2018). Recent breakthroughs and ongoing limitations in *Cryptosporidium* research. *F1000Res.* 7, F1000 Faculty Rev-1380.
  10. Manjunatha, U.H., Vinayak, S., Zambriski, J.A., Chao, A.T., Sy, T., Noble, C.G., Bonamy, G.M.C., Kondreddi, R.R., Zou, B., Gedeck, P., et al. (2017). A *Cryptosporidium* P(4)K inhibitor is a drug candidate for cryptosporidiosis. *Nature* 546, 376–380.
  11. Vinayak, S., Pawlowic, M.C., Sateriale, A., Brooks, C.F., Studstill, C.J., Bar-Peled, Y., Cipriano, M.J., and Striepen, B. (2015). Genetic modification of the diarrhoeal pathogen *Cryptosporidium parvum*. *Nature* 523, 477–480.
  12. Guérin, A., and Striepen, B. (2020). The biology of the intestinal intracellular parasite *Cryptosporidium*. *Cell Host Microbe* 28, 509–515.
  13. Tandel, J., English, E.D., Sateriale, A., Gullicksrud, J.A., Beiting, D.P., Sullivan, M.C., Pinkston, B., and Striepen, B. (2019). Life cycle progression and sexual development of the apicomplexan parasite *Cryptosporidium parvum*. *Nat. Microbiol.* 4, 2226–2236.
  14. Bhalchandra, S., Lamisere, H., and Ward, H. (2020). Intestinal organoid/enteroid-based models for *Cryptosporidium*. *Curr. Opin. Microbiol.* 58, 124–129.
  15. Clevers, H. (2016). Modeling development and disease with organoids. *Cell* 165, 1586–1597.
  16. Aguilar, C., Alves da Silva, M., Saraiva, M., Neyazi, M., Olsson, I.A.S., and Bartfeld, S. (2021). Organoids as host models for infection biology—a review of methods. *Exp. Mol. Med.* 53, 1471–1482.
  17. Heo, I., Dutta, D., Schaefer, D.A., Iakobachvili, N., Artegiani, B., Sachs, N., Boonekamp, K.E., Bowden, G., Hendrickx, A.P.A., Willems, R.J.L., et al. (2018). Modelling *Cryptosporidium* infection in human small intestinal and lung organoids. *Nat. Microbiol.* 3, 814–823.
  18. Wilke, G., Funkhouser-Jones, L.J., Wang, Y., Ravindran, S., Wang, Q., Beatty, W.L., Baldrige, M.T., VanDussen, K.L., Shen, B., Kuhlenschmidt, M.S., et al. (2019). A stem-cell-derived platform enables complete *Cryptosporidium* development *in vitro* and genetic tractability. *Cell Host Microbe* 26, 123–134.e8.
  19. Greigert, V., Saraav, I., Son, J., Zhu, Y., Dayao, D., Antia, A., Tzipori, S., Witola, W.H., Stappenbeck, T.S., Ding, S., and Sibley, L.D. (2024). *Cryptosporidium* infection of human small intestinal epithelial cells induces type III interferon and impairs infectivity of rotavirus. *Gut Microb.* 16, 2297897.
  20. Jaskiewicz, J.J., Sandlin, R.D., Swei, A.A., Widmer, G., Toner, M., and Tzipori, S. (2018). Cryopreservation of infectious *Cryptosporidium parvum* oocysts. *Nat. Commun.* 9, 2883.
  21. Jaskiewicz, J.J., Sevenler, D., Swei, A.A., Widmer, G., Toner, M., Tzipori, S., and Sandlin, R.D. (2020). Cryopreservation of infectious *Cryptosporidium parvum* oocysts achieved through vitrification using high aspect ratio specimen containers. *Sci. Rep.* 10, 11711.
  22. Jaskiewicz, J.J., Dayao, D.A.E., Girouard, D., Sevenler, D., Widmer, G., Toner, M., Tzipori, S., and Sandlin, R.D. (2023). Scalable cryopreservation of infectious *Cryptosporidium hominis* oocysts by vitrification. *PLoS Pathog.* 19, e1011425.
  23. Guérin, A., Strelau, K.M., Barylyuk, K., Wallbank, B.A., Berry, L., Crook, O.M., Lilley, K.S., Waller, R.F., and Striepen, B. (2023). *Cryptosporidium* uses multiple distinct secretory organelles to interact with and modify its host cell. *Cell Host Microbe* 31, 650–664.e6.
  24. Wang, L., Wang, Y., Cui, Z., Li, D., Li, X., Zhang, S., and Zhang, L. (2022). Enrichment and proteomic identification of *Cryptosporidium parvum* oocyst wall. *Parasites Vectors* 15, 335.
  25. Morada, M., Lee, S., Gunther-Cummins, L., Weiss, L.M., Widmer, G., Tzipori, S., and Yarlett, N. (2016). Continuous culture of *Cryptosporidium parvum* using hollow fiber technology. *Int. J. Parasitol.* 46, 21–29.
  26. DeCicco RePass, M.A., Chen, Y., Lin, Y., Zhou, W., Kaplan, D.L., and Ward, H.D. (2017). Novel bioengineered three-dimensional human intestinal model for long-term infection of *Cryptosporidium parvum*. *Infect. Immun.* 85, e00731-16.
  27. Jia, R., Huang, W., Huang, N., Yu, Z., Li, N., Xiao, L., Feng, Y., and Guo, Y. (2022). High infectivity and unique genomic sequence characteristics of *Cryptosporidium parvum* in China. *PLoS Neglected Trop. Dis.* 16, e0010714.
  28. Wang, T., Guo, Y., Roellig, D.M., Li, N., Santín, M., Lombard, J., Kváč, M., Naguib, D., Zhang, Z., Feng, Y., and Xiao, L. (2022). Sympatric recombination in zoonotic *Cryptosporidium* leads to emergence of populations with modified host preference. *Mol. Biol. Evol.* 39, 150.
  29. Huang, W., He, W., Tang, Y., Chen, M., Sun, L., Yang, Z., Hou, T., Liu, H., Chen, H., Wang, T., et al. (2023). Unique genomic characteristics underlie the infectivity of divergent *Cryptosporidium hominis* subtypes to animals. Preprint at Research Square. [https://doi.org/10.21203/rs-3617590/v3617591](https://doi.org/10.21203/rs.21203.rs-3617590/v3617591).
  30. He, X., Huang, W., Sun, L., Hou, T., Wan, Z., Li, N., Guo, Y., Kváč, M., Xiao, L., and Feng, Y. (2022). A productive immunocompetent mouse model of cryptosporidiosis with long oocyst shedding duration for immunological studies. *J. Infect.* 84, 710–721.
  31. Korpe, P.S., Valencia, C., Haque, R., Mahfuz, M., McGrath, M., Houpt, E., Kosek, M., McCormick, B.J.J., Penataro Yori, P., Babji, S., et al. (2018). Epidemiology and risk factors for cryptosporidiosis in children from 8 low-income sites: results from the MAL-ED study. *Clin. Infect. Dis.* 67, 1660–1669.
  32. Borowski, H., Thompson, R.C.A., Armstrong, T., and Clode, P.L. (2010). Morphological characterization of *Cryptosporidium parvum* life-cycle stages in an *in vitro* model system. *Parasitology* 137, 13–26.
  33. Sun, L., Li, J., Xie, F., Wu, S., Shao, T., Li, X., Li, J., Jian, F., Zhang, S., Ning, C., et al. (2022). Whole transcriptome analysis of HCT-8 cells infected by *Cryptosporidium parvum*. *Parasites Vectors* 15, 441.
  34. Rossi, P., Pozio, E., and Besse, M.G. (1990). Cryopreservation of *Cryptosporidium* sp. oocysts. *Trans. R. Soc. Trop. Med. Hyg.* 84, 68.
  35. Fayer, R., Nerad, T., Rall, W., Lindsay, D.S., and Blagburn, B.L. (1991). Studies on cryopreservation of *Cryptosporidium parvum*. *J. Parasitol.* 77, 357–361.
  36. Kim, H.C., and Healey, M.C. (2001). Infectivity of *Cryptosporidium parvum* oocysts following cryopreservation. *J. Parasitol.* 87, 1191–1194.
  37. Paziewska-Harris, A., Schoone, G., and Schallig, H.D.F.H. (2018). Long-term storage of *Cryptosporidium parvum* for *in vitro* culture. *J. Parasitol.* 104, 96–100.
  38. Li, N., Zhao, W., Song, S., Ye, H., Chu, W., Guo, Y., Feng, Y., and Xiao, L. (2022). Diarrhoea outbreak caused by coinfections of *Cryptosporidium parvum* subtype IIdA20G1 and rotavirus in pre-weaned dairy calves. *Transboundary Emerg. Dis.* 69, e1606–e1617.
  39. Pawlowic, M.C., Vinayak, S., Sateriale, A., Brooks, C.F., and Striepen, B. (2017). Generating and maintaining transgenic *Cryptosporidium parvum* parasites. *Curr. Protoc. Microbiol.* 46, 20B.22.21–20B.22.32.
  40. Chen, L., Hu, S., Jiang, W., Zhao, J., Li, N., Guo, Y., Liao, C., Han, Q., Feng, Y., and Xiao, L. (2019). *Cryptosporidium parvum* and *Cryptosporidium hominis* subtypes in crab-eating macaques. *Parasites Vectors* 12, 350.
  41. Li, N., Neumann, N.F., Ruecker, N., Alderisio, K.A., Sturbaum, G.D., Villegas, E.N., Chalmers, R., Monis, P., Feng, Y., and Xiao, L. (2015). Development and evaluation of three real-time PCR assays for genotyping and source tracking *Cryptosporidium* spp. in water. *Appl. Environ. Microbiol.* 81, 5845–5854.
  42. Feng, Y., Li, N., Duan, L., and Xiao, L. (2009). *Cryptosporidium* genotype and subtype distribution in raw wastewater in Shanghai, China: evidence for possible unique *Cryptosporidium hominis* transmission. *J. Clin. Microbiol.* 47, 153–157.

## STAR★METHODS

### KEY RESOURCES TABLE

REAGENT or RESOURCE	SOURCE	IDENTIFIER
<b>Antibodies</b>		
Crypt-a-Glo	Waterborne	Cat#A400FLR-20X
Sporo-Glo	Waterborne	Cat#A600Cy3R-20X
mouse anti-villin	Abcam	Cat#AB97512; RRID: AB_10680291
rabbit anti-mucin 2	Abcam	Cat#AB272692; RRID: AB_2888616
goat anti-mouse IgG Alexa Fluor 488	Abcam	Cat#AB150077; RRID: AB_2630356
rabbit anti-Ki-67	Servicebio	Cat#GB111141
goat anti-rabbit IgG Alexa Fluor 568	Invitrogen	Cat#A11011; RRID: AB_143157
Rabbit anti-Cp	homemade	Cat#N/A
<b>Chemicals, peptides, and recombinant proteins</b>		
Y-27632 dihydrochloride ROCK inhibitor	Tocris	Cat#1254
Glutamax	Gibco	Cat#35050061
HEPES	Gibco	Cat#15630-808
Penicillin/Streptomycin	Gibco	Cat#15140122
N2	Gibco	Cat#A1370701
B27	Gibco	Cat#12587-0101
Gentamicin	Bioss	Cat#C7011
mEGF	SinoBiological	Cat#50482-MNCH
Primocin	InvivoGen	Cat#ant-pm-1
Nicotinamide	Sigma	Cat#N0636
Matrigel	BD	Cat#356234
Gentle Cell Dissociation Reagent	STEMCELL	Cat#07174
Fetal bovine serum	Gibco	Cat#10099141
TrypLE Express	Gibco	Cat#12604-013
Mitomycin C	CST	Cat#51854S
CryStor CS10	STEMCELL	Cat#07930
BSA	Biofrox	Cat#4240GR100
4% paraformaldehyde	Leagene	Cat#DF0135
Triton X-100	Sigma	Cat#9002-93-1
DAPI	CST	Cat# 4083S
Advanced DMEM/F-12	Gibco	Cat#12634-010
DMEM	Gibco	Cat#c11995500bt
DMEM/F-12	Gibco	Cat#11320033
<b>Critical commercial assays</b>		
QIAamp DNA Mini kit	QIAGEN	Cat#51306
FastDNA SPIN Kit for Soil	MP Biomedicals	Cat#116560200
<b>Deposited data</b>		
RNA-seq data	This paper	PRJNA988932
<b>Experimental models: Cell lines</b>		
Mouse: NIH/3T3	ATCC	CRL-1658
Mouse: L-WRN	ATCC	CRL-3276

(Continued on next page)

**Continued**

REAGENT or RESOURCE	SOURCE	IDENTIFIER
Human: HCT-8	ATCC	CCL-244
Mouse: enteroids	This paper	N/A
<b>Experimental models: Organisms/strains</b>		
<i>Cryptosporidium parvum</i> Ila-Waterborne (IlaA17G2R1 subtype)	Waterborne	N/A
<i>Cryptosporidium parvum</i> IId-HLJ isolate (IIdA20G1 subtype)	State Key Laboratory for Animal Disease Control and Prevention	N/A
<i>Cryptosporidium hominis</i> Ib isolate (IbA12G3 subtype)	State Key Laboratory for Animal Disease Control and Prevention	N/A
<i>Cryptosporidium hominis</i> Im isolate (ImA20 subtype)	State Key Laboratory for Animal Disease Control and Prevention	N/A
<i>Cryptosporidium hominis</i> In isolate (InA17 subtype)	State Key Laboratory for Animal Disease Control and Prevention	N/A
Mouse: Infg KO (C57BL/6 background)	State Key Laboratory for Animal Disease Control and Prevention	N/A
<b>Oligonucleotides</b>		
Primer: 18S-LC2 forward: AAGTATAAACCCCTTTACAAGTA	30	N/A
Primer: 18S-LC2 reverse: TATTATTCCATGCTGGAGTATTC	30	N/A
<b>Software and algorithms</b>		
Fiji	ImageJ	<a href="https://fiji.sc/">https://fiji.sc/</a>
CellSens Standard1 software	Olympus	N/A
<b>Deposited data</b>		
The original data generated in this work has been deposited in Mendeley Data	This work	Mendeley Data: <a href="https://data.mendeley.com/datasets/5n8v8fsncr/1">https://data.mendeley.com/datasets/5n8v8fsncr/1</a>
The RNA-seq data generated in this study have been deposited in the SRA database of the National Center for Biotechnology Information	This work	SRA: PRJNA988932 ( <a href="https://www.ncbi.nlm.nih.gov/sra/PRJNA988932">https://www.ncbi.nlm.nih.gov/sra/PRJNA988932</a> )
<b>Other</b>		
NovaSeq 6000 sequencing system	Illumina	N/A
EVO MA 15/LS 15	Zeiss	N/A
Talos L120C	Thermo Fisher	N/A
Olympus BX53	Olympus	N/A
40 $\mu$ m filter	Corning	Cat#352340
70 $\mu$ m filter	Corning	Cat#352350
3 $\mu$ m filters	Whatman	Cat#110612
Transwell 24 well plate (polyestermembrane with 0.4 $\mu$ m pores)	Biofil	Cat#TCS012024
Roche LightCycler 480 II	Roche	N/A

**RESOURCE AVAILABILITY**

**Lead contact**

Further information and requests for resources and reagents should be directed to and will be fulfilled by the Lead Contact, Lihua Xiao ([lxiao1961@gmail.com](mailto:lxiao1961@gmail.com)).

### Materials availability

This study did not generate new unique reagents.

### Data and code availability

Original data have been deposited at Mendeley Data (<https://data.mendeley.com/>) and the RNA-seq data generated in this study have been deposited in the SRA database of the National Center for Biotechnology Information. These data are publicly available as of the date of publication and the accession number is listed in the [key resources table](#). This paper does not report original code. Any additional information required to reanalyze the data reported in this paper is available from the [lead contact](#) upon request.

## EXPERIMENTAL MODEL AND STUDY PARTICIPANT DETAILS

### Cryptosporidium isolates

The Ila-Waterborne isolate (designated as the IOWA isolate but belonged to the IlaA17G2R1 subtype) of *C. parvum* was purchased from Waterborne, Inc. The IId-HLJ isolate of the IIdA20G1 subtype was initially obtained from a dairy calf on a farm in Heilongjiang (HLJ), China and maintained through passages in GKO mice.<sup>27,38</sup> This isolate has higher infectivity and some unique genomic sequence characteristics in comparison with the IlaA17G2R1-Waterborne isolate as previously described.<sup>27</sup> Oocysts of nonhuman primate-adapted *C. hominis* isolates of the Iba12G3, Ima20, Ina17 subtypes were initially obtained from crab-eating macaques (*Macaca fascicularis*) in China using sucrose and cesium chloride gradient centrifugations.<sup>39,40</sup> In a separate study, comparative genomic analysis of the three macaque *C. hominis* isolates and common *C. hominis* isolates from humans confirmed their *C. hominis* identity, with 16315-16709 SNPs from common *C. hominis* (compared to ~20000 SNPs between the anthroponotic IId and zoonotic Ila or IId *C. parvum*).<sup>29</sup> They have two subtelomeric MEDLE genes and one subtelomeric INS gene that are usually found only in *C. parvum*. In experimental infection of GKO mice, the three macaque isolates induced high levels of oocyst shedding (> 10<sup>6</sup> OPG) and long oocyst shedding duration (> 80 days).<sup>29</sup> These three unique *C. hominis* isolates have been maintained in our laboratory through passages in GKO mice since their initial isolation in August 2020, with subtype confirmation after each passage. All *C. parvum* and *C. hominis* oocysts used in the study were recovered from mouse feces using a discontinuous sucrose and cesium chloride gradient as previously described.<sup>27</sup> The purified oocysts were stored in PBS with antibiotics at 4°C for less than two months before use.

### Mice

Six-week-old female C57BL/6 mice were used for the establishment of enteroids. Specific-pathogen-free GKO mice with a C57BL/6 background at age four weeks were used in assessment of the infectivity of oocysts produced in culture. Mice were housed individually and supplied with sterilized diet, water, and bedding. The study was conducted in compliance with the Guide for the Care and Use of Laboratory Animals. The research protocol was approved by the Committee on the Ethic Use of Animals in Research, South China Agricultural University (No. 2023F098).

## METHOD DETAILS

### Establishment and maintenance of enteroids

Ileum crypts were isolated from 6-week-old female C57BL/6 mice. Two to three sections (~4 cm) were harvested from the small intestine of sacrificed mice, opened longitudinally, and washed with ice-cold PBS three times. They were cut into 2~3 mm pieces and rotated in a 15 ml tube at 4°C and 20 rpm in EDTA chelation buffer (ice-cold PBS containing 2 mM EDTA and 100 mg/ml gentamicin) for 40 min. The tissue fragments were allowed to settle on ice for 30 sec. After replacing the buffer with ice-cold PBS (~5 ml), the tube was shaken violently until the supernatant was clouded. The tissue suspension was filtered through a pre-wetted 70 µm filter (Corning) to collect the filtrate. This procedure was repeated 3~4 times, and the pooled filtrate was centrifuged at 4°C and 300 g for 5 min. Crypts in the tube were collected after removing the supernatant, and resuspended in 50% L-WRN conditioned medium (CM, Table S3) mixed 1:1 with Matrigel (BD Biosciences). The crypt suspension (55 µl per well) was transferred into a pre-warmed 24-well plate, and incubated at 37°C for 10 min to congeal the Matrigel. Afterwards, 700 µl CM was added into each well gently, not disturbing the Matrigel domes. The plate was incubated at 37°C and 5% CO<sub>2</sub>, with the medium being replaced with fresh CM every 2~3 days. The enteroids were passaged after 7 days by the addition of 1 ml Gentle Cell Dissociation Reagent (STEMCELL) and repeated pipetting to break up the enteroid-Matrigel domes. The suspension was digested at room temperature for 10 min and centrifuged at 4°C and 300 g for 5 min. After removing the supernatant, the enteroids were washed with 1 ml DMEM/F-12 by centrifugation. Aliquots of the enteroids were mixed with Matrigel, plated into a pre-warmed 24-well plate, and cultured as described above. We passaged enteroids using the 1:4 split ratio every 3 or 4 days.

NIH/3T3 embryonic mouse fibroblast cells (ATCC, CRL-1658) were cultured at 37°C and 5% CO<sub>2</sub> in DMEM (Gibco) supplemented with 10% fetal bovine serum (FBS, Gibco) and 1U/ml penicillin/streptomycin, and passaged every 2 days in a 1:5 split.

### Generation of ALI culture system and infection with *Cryptosporidium* spp

The procedures described in the previous study<sup>18</sup> were used in the generation of the ALI culture system, with the following modifications: 1) we treated the i3T3 cells with mitomycin C instead of irradiation; 2) we changed the digestion of enteroids from the use of trypsin solution to a

more gentle approach (using TrypLE Express) to reduce damages to the enteroid cells; 3) we supplemented the CM with additional growth factors and antibiotics such as mouse EGF and Primocin (Table S3).

For the construction of the ALI system, 3T3 cells were incubated in 4  $\mu\text{g}/\text{ml}$  mitomycin C (CST, cat# 51854S) for 1 h and washed three times with PBS to create i3T3 cells as the feeder cells. The i3T3 cells were plated at the density of  $8 \times 10^4$  i3T3 cells on a Transwell insert (polyester membrane with 0.4  $\mu\text{m}$  pores; Biofil, 12 Transwells per 24-well plate) that was pre-coated with diluted Matrigel (Matrigel: ice-cold PBS=1:10). DMEM with 10% FBS and 1U/ml penicillin/streptomycin was added to the top (100  $\mu\text{l}$ ) and bottom (400  $\mu\text{l}$ ) parts of the Transwell and incubated at 37°C and 5% CO<sub>2</sub> for approximately 24 h. The next day, the enteroids were trypsinized using TrypLE Express (Gibco) and roughly pipetted. After 10 min digestion at room temperature, the cells were centrifuged at 300 g for 5 min and washed with DMEM/F-12. The cells were re-suspended in 1 ml CM and filtered through a pre-wetted 40  $\mu\text{m}$  filter (Corning) to remove undigested enteroids, and seeded on the i3T3 cell layers with  $5 \times 10^4$  cells per Transwell. The medium in the top (200  $\mu\text{l}$ ) and bottom (400  $\mu\text{l}$ ) parts of Transwell was changed every 2 days as described above. To create the ALI for cell differentiation, the medium in the top chamber of the Transwell was removed at day 7 of the culture, while the medium in the bottom chamber was changed every 2 days. Three days after removing the top medium, the ALI system was infected with oocysts or purified sporozoites as described previously<sup>18</sup> (Figure 1A). Briefly, oocysts were treated with 8.25% sodium hypochlorite (diluted in PBS) for 10 min on ice, and washed three times in PBS with 1% BSA. In some experiments, oocysts were excysted and the released sporozoites were used for infection. Oocysts were excysted by incubation in 0.75% sodium taurocholate (diluted in PBS with 1% BSA) in a 37°C water bath for 60-90 min. Released sporozoites were collected from excystation suspensions using 3  $\mu\text{m}$  filters (Whatman) and washed in PBS with 1% BSA. For infection of ALI cultures, oocysts or sporozoites were suspended in CM and added to the upper chamber of each Transwell (100  $\mu\text{l}$  per well) for 2 hours. The chamber was washed three times with PBS containing 1% BSA to remove extracellular parasites and restore the air-liquid interface. For infection of HCT-8 cultures, oocysts or sporozoites were suspended in medium and added directly to the culture for 2 hours.

### Cryopreservation of *C. parvum*-infected ALI or HCT-8 cultures

Cryopreservation was performed on ALI cultures (at 6 h or 12 h) or HCT-8 cells (at 6 h) infected with sporozoites purified by using 3  $\mu\text{m}$  filters. ALI cultures were infected with *C. parvum* as described above ( $\sim 4 \times 10^5$  sporozoites per Transwell), whereas HCT-8 cultures were infected by adding purified sporozoites ( $\sim 8 \times 10^5$  sporozoites per well in 48-well plates) into the medium of HCT-8 cells. For cryopreservation, cells from 2~3 Transwells (for ALI cultures) or one well of 48-well plates (for HCT-8 cultures) were placed into each cryovial (1 ml). Prior to the collection of culture materials, the culture medium was replaced with ice-cold PBS, and the cultures infected with *C. parvum* were pipetted repeatedly. After centrifugation at 4°C and 300 g for 5 min and one wash with DMEM/F-12, the cells harvested were resuspended in cryovials with 1 ml of cryoprotectant (CryStor CS10, containing 10% dimethyl sulfoxide, STEMCELL) for the cryopreservation of organoids. After storage in a freezing container at -80°C for 24 h, the cryovials were transferred to liquid nitrogen for long-term storage.

For thawing the frozen cultures, cryovials were placed in a 37°C water bath for 2~2.5 min. When the freezing medium became liquid, the cells infected with parasites were transferred immediately to 15-ml tubes containing 3 ml DMEM/F-12 with 1% BSA (Biofrox). After careful mixing, the cell suspension was centrifuged at 4°C and 200 g for 5 min to remove the cryoprotectant. After removing the supernatant, the intracellular parasites were resuspended with 0.5 ml CM and seeded into 1~2 Transwells in ALI cultures. The infected ALI cultures were maintained as described above.

### Measurement of *Cryptosporidium* growth

In measurement of *Cryptosporidium* growth in the ALI system, three wells of cultures were used for each infection group at each sampling point. DNA was extracted from each well using the QIAamp DNA Mini kit (Qiagen) after five freeze-thaw cycles in liquid-nitrogen and 56°C water-bath. In measurement of *Cryptosporidium* shedding in GKO mice, DNA was extracted from 0.1 g fecal pellets from each mouse using the FastDNA SPIN Kit for Soil (MP Biomedicals). The infection intensity in Transwells and mice was assessed using SYBR Green-based 18S-LC2 qPCR as described.<sup>41</sup> Student's t-test was used to compare the parasite burden between groups. Differences were considered significant at  $P < 0.05$ .

### Microscopic analyses of ALI cultures

For immunostaining, monolayers in the Transwell inserts were fixed with 0.2 ml 4% paraformaldehyde for 10 min, permeabilized with 0.1% Triton X-100 (Sigma) for 10 min, and blocked with 1% BSA for 60 min. The cells were then incubated at room temperature with Crypt-a-Glo (Waterborne, 1:20) and Sporo-Glo (Waterborne, 1:20) for 60 min. DAPI (CST, DAPI: PBS = 1:2 000) was used to stain the nuclear DNA. The membrane of the Transwell insert was cut with a scalpel and plated on a glass slide for microscopy.

For histological analyses, Transwells were fixed at room temperature by adding 4% paraformaldehyde into both the top (0.2 ml) and bottom (0.4 ml) chambers for 30 min. The Transwell membranes were cut from the inserts using a scalpel and processed for paraffin embedding. Sections of 4  $\mu\text{m}$  in thickness were cut and stained with conventional procedures for the hematoxylin and eosin (H&E) staining and immunohistochemistry. The primary antibodies used in immunofluorescence analysis included mouse anti-villin (1:1000, Abcam), rabbit anti-mucin 2 (1:1000, Abcam) and rabbit anti-Ki-67 (1:500, Servicebio), while the secondary antibodies included goat anti-mouse IgG Alexa Fluor 488 (Abcam) and goat anti-rabbit IgG Alexa Fluor 568 (Invitrogen).

The slides generated were examined under an Olympus BX53 (Olympus, Japan) fluorescence microscope. Images were acquired using the CellSens Standard1 software (Olympus) and processed in ImageJ or Photoshop.

For ultrastructural analyses, ALI monolayers were fixed with 2.5% glutaraldehyde and processed for SEM and TEM using conventional procedures. They were examined under an EVO MA 15/LS 15 (Carl Zeiss Microscopy GmbH, Jena, Germany) and Talos L120C (Thermo Fisher, Waltham, USA), respectively.

### Experimental infection of GKO mice with cultured parasites

For the assessment of the infectivity of oocysts produced from ALI system without cryopreservation, three or four GKO mice ( $n = 3$  or  $4$ ) were orally gavaged with 200  $\mu$ l of bleach-treated ALI material (equivalent to 1.25 Transwells per mouse) harvested one (D1) or three (D3) days after the infection with sporozoites. For the assessment of the infectivity of oocysts produced from the ALI system after cryopreservation, GKO mice were pretreated with 1 mg/ml ampicillin (Macklin), 1 mg/ml streptomycin (Macklin) and 0.5 mg/ml vancomycin (Macklin) for three days before infection. Each mouse in the infection group ( $n = 3$ ) was infected with cell materials of 2~3 Transwells, which contained ALI cultures infected with recovered parasites for 4 days. In contrast, mice in the control group ( $n = 3$ ) were gavaged with PBS. Fecal samples were collected from each mouse every three days for the measurement of oocyst shedding using a 18S-LC2 qPCR as described above. The subtype identity of the oocysts shedding in GKO mice was confirmed by sequence analysis of the *gp60* gene as described.<sup>42</sup>

### RNA-seq analysis of *C. hominis*-infected ALI and HCT-8 cultures

RNA was isolated from uninfected and *C. hominis*-infected Transwell cultures or HCT-8 cells 72 hours after the infection. ALI cultures in each of the eight Transwells were infected with  $4 \times 10^5$  Ib sporozoites, with eight wells of uninfected cultures used as controls. To obtain sufficient RNA for sequencing, two Transwells were pooled as one sample. For the RNA-seq analysis of HCT-8 cultures, HCT-8 cells in each of four wells (in a 48-well plate) were infected with  $8 \times 10^5$  Ib sporozoites, with four wells of uninfected cultures used as controls. The monolayer obtained from each well was counted as one sample. For this, 0.5 ml ice-cold PBS was used to harvest the monolayers by centrifugation at 4°C and 300 g for 5 min. After removing the supernatant, 0.2 ml of Trizol was added into each sample and pipetted several times until the suspension became opaque. The samples were frozen in liquid-nitrogen immediately and stored at -80°C before RNA-seq using the Illumina NovaSeq 6000 at Guangzhou Genedenovo Biotechnology Co. Transcriptomic analysis of the RNA-seq data for host cell responses and *C. hominis* gene expression was performed as described previously.<sup>30</sup> Briefly, the raw sequence reads were assessed for quality control using FastQC v0.11.2. Adapter and low-quality sequences were trimmed using Trimmomatic v0.39. Clean reads were mapped to the reference genomes using default parameters by using STAR v2.7.6a. Expression matrices were generated using RSEM v1.3.3 of the RNA-seq data. The “DESeq2” package in R v4.1.0 was used to compare data from the infection and control groups at different oocyst shedding times. DEGs were identified by absolute fold change  $> 2$  and  $P$  values  $< 0.05$ . KEGG and GO analyses of DEGs were used to identify biological pathways and terms involved.

### QUANTIFICATION AND STATISTICAL ANALYSIS

Statistical analysis was done using GraphPad Prism. The information about plot type, error bars, number of replicates and  $P$  values can be found in the figure legends.